

Degradable thiol-acrylate hydrogels as tunable matrices for three-dimensional hepatic culture

Yiting Hao, Chien-Chi Lin

Department of Biomedical Engineering, Purdue School of Engineering and Technology, Indiana University-Purdue University Indianapolis, Indianapolis, Indiana 46202

Received 18 September 2013; revised 8 November 2013; accepted 26 November 2013

Published online 13 December 2013 in Wiley Online Library (wileyonlinelibrary.com). DOI: 10.1002/jbm.a.35044

Abstract: A degradable poly(ethylene glycol)-diacrylate (PEGDA) hydrogel system was developed using simple macromer formulations and visible light initiated thiol-acrylate photopolymerization. In addition to PEGDA, other components in this gelation system include eosin-Y as a photosensitizer, bi-functional thiol (dithiothreitol, DTT) as a dual-purpose co-initiator and cross-linker, and *N*-vinylpyrrolidone (NVP) as a co-monomer. Gelation was achieved through a mixed-mode step-chain growth polymerization mechanism under bright visible light exposure. Increasing photosensitizer or NVP concentrations accelerated photocrosslinking and increased final gel stiffness. Increasing bi-functional thiol content in the prepolymer solution only increased gel stiffness to some degree. As the concentration of thiol surpassed certain range, thiol-mediated chain-transfer events caused thiol-acrylate gels to form with lower degree of cross-linking. Pendant peptide, such as integrin ligand RGDS, was more effectively immobilized in the network via a thiol-acrylate reaction (using thiol-bearing peptide Ac-CRGDS. Underline indicates cross-linkable motif) than through homopolymerization of acrylated peptide (e.g., acryl-RGDS). The

incorporation of pendant peptide comes with the expense of a lower degree of gel cross-linking, which was rectified by increasing co-monomer NVP content. Without the use of any readily degradable macromer, these visible light initiated mixed-mode cross-linked hydrogels degraded hydrolytically due to the formation of thiol-ether-ester bonds following thiol-acrylate reactions. An exponential growth relationship was identified between the hydrolytic degradation rate and bifunctional thiol content in the prepolymer solution. Finally, we evaluated the cytocompatibility of these mixed-mode cross-linked degradable hydrogels using *in situ* encapsulation of hepatocellular carcinoma Huh7 cells. Encapsulated Huh7 cells remained alive and proliferated as time to form cell clusters. The addition of NVP at a higher concentration (0.3%) did not affect Huh7 cell viability but resulted in reduction of cell metabolic activity, which was accompanied by an elevated urea secretion from the encapsulated cells. © 2013 Wiley Periodicals, Inc. *J Biomed Mater Res Part A*: 102A: 3813–3827, 2014.

Key Words: visible light, photopolymerization, thiol-acrylate, hydrogels, hepatocyte

How to cite this article: Hao Y, Lin C-C. 2014. Degradable thiol-acrylate hydrogels as tunable matrices for three-dimensional hepatic culture. *J Biomed Mater Res Part A* 2014;102A:3813–3827.

INTRODUCTION

Hydrogels prepared from derivatives of poly(ethylene glycol) (PEG) have been employed in a wide variety of controlled release, drug delivery, and tissue regeneration applications.^{1–4} Linear or multi-arm PEG-based macromers with reactive termini are increasingly being developed for hydrogel preparation. The reactive terminal groups render the otherwise soluble PEG cross-linkable while the hydrophilic and non-fouling nature of PEG backbone affords high cytocompatibility and biocompatibility needed in biomedical applications. Some of the commonly used functional termini include acrylate, methacrylate, acrylamide, maleimide, norbornene, allylether, azide, alkyne, tetrazine, etc. The mechanism by which PEG macromers cross-link into hydrogels depends on the reactivity of the terminal functional groups.

For example, PEG-diacrylate (PEGDA) or PEG-dimethacrylate (PEGDM) can be cross-linked into hydrogels by means of chain-growth polymerization with the use of appropriate initiators.⁵ On the other hand, multi-arm PEG-maleimide or PEG-acrylate reacts readily with multifunctional thiol-terminated linkers via a nucleophilic step-growth cross-linking mechanism.⁶ Recently, research efforts have focused on creating 'clickable' PEG-based macromers that form hydrogels through bio-orthogonal reactions without catalyst or external stimuli.^{7–9}

Although PEG-based macromers are increasingly being developed for biomedical applications, PEG-di(meth)acrylate (PEGDA or PEGDM) continues to be among the most highly used macromers in hydrogel fabrication due to the simplicity of macromer synthesis and the high availability of these

Correspondence to: C.-C. Lin; e-mail: lincc@iupui.edu

Contract grant sponsor: IUPUI Biomechanics and Biomaterials Research Center (BBRC Pilot project) and IUPUI Department of Biomedical Engineering (Faculty start-up fund)

macromers from various commercial sources.^{10–19} One of the most commonly used cross-linking methods for forming PEGDA hydrogel is through radical-mediated photopolymerization. In one classic example, a type I photoinitiator (e.g., Irgacure 2959) is cleaved into two radical species upon exposure of long wavelength ultraviolet (UV) light.¹¹ The radicals generated from initiator molecules propagate through acrylate moieties on PEGDA to form a cross-linked hydrogel network. While this method is simple and allows for rapid and spatial-temporally controlled gelation kinetics, the use of UV light often raises concerns in clinically relevant settings. Another drawback is that I-2959 is only marginally soluble in aqueous solution (<0.5 wt %) and has very low molar absorptivity in cyto-compatible UV wavelength ($\epsilon \sim 10M^{-1}cm^{-1}$ at 365 nm). In view of the potential cytotoxicity of UV light, photoinitiators sensitive to visible light can be used to initiate gel cross-linking. For example, a highly water-soluble (>5 wt %) photoinitiator lithium arylphosphinate (LAP) has been utilized to initiate gel cross-linking.²⁰ While LAP can also be cleaved by visible light at 405 nm, its molar absorptivity at this wavelength is relatively low ($\epsilon \sim 30M^{-1}cm^{-1}$).²¹ Furthermore, the cleavage of LAP under light exposure still creates additional radical species that are harmful to radical sensitive cells.

Visible light initiated gelation can also be achieved using a type II (non-cleavage type) initiator, such as eosin-Y.^{12,19,22–25} Although these initiators (or photosensitizers) have exceptionally high molar absorptivity in the visible light range (e.g., $\epsilon > 10^6M^{-1}cm^{-1}$ for eosin-Y at 515 nm), they cannot initiate polymerization without a co-initiator. One of the commonly used co-initiators is triethanolamine (TEA), which is typically used at a submolar and cytotoxic concentration (30–225 mM).^{12,19,22–25} To accelerate gelation, a small molecular weight co-monomer *N*-vinylpyrrolidone (NVP) is also routinely added in the prepolymer solution.^{12,22,26} Rapid gelation can be achieved by fine-tuning the concentrations of these three components (i.e., eosin-Y, TEA, NVP). Although this gelation scheme has enjoyed various degrees of success in preparing hydrogels for cell surface coating, *in situ* cell encapsulation, and drug delivery applications,^{19,27,28} the use of high concentration of cytotoxic TEA largely offset the benefits of cyto-compatible visible light.²⁹ Furthermore, chain-growth PEGDA hydrogels prepared by UV light or current visible light initiated cross-linking methods do not degrade readily, unless the PEG macromers are modified chemically with cleavable segments before network cross-linking.^{5,19,30–32}

Effective immobilization of bioactive motifs (e.g., integrin-binding or protein-sequestering ligands) within the otherwise inert PEG-based hydrogel is also of paramount importance. The most commonly used method to render bioactive ligands (e.g., peptides, proteins, nucleic acid aptamer, etc.) cross-linkable in PEGDA hydrogels is through modifying the ligand with acrylate functionality.¹⁰ Following chain-growth polymerization, the acrylated ligands are immobilized in the polyacrylate kinetic chains, which may create steric hindrance and decrease the accessibility for the binding partners (e.g., cell surface receptors, soluble growth

factors, etc.).^{18, 33} It has also been shown that the immobilization efficiency of acrylated pendant ligands in a PEGDA network was relatively low (23%–66%).^{12, 22} Further, when utilizing peptides/proteins with bioactive primary amine groups, this method may be problematic because acrylation most often takes place on the bioactive primary amine groups.¹⁰ Alternative, pendant ligands can be immobilized in PEGDA hydrogels via thiolation or site-specific cysteine insertion, followed by a mixed-mode thiol-acrylate polymerization for immobilization.^{17,34} Since the immobilization of thiolated ligand in a PEGDA network is through a step-growth reaction, the immobilized ligand is less likely to experience steric hindrance. Furthermore, studies have shown that thiol-acrylate mixed-mode polymerization mechanism affords high ligand immobilization efficiency (~90%).¹⁷ A major concern with mixed-mode ligand immobilization is that the thiol-ether-ester linkage formed after the thiol-acrylate step-growth reaction may be slowly hydrolyzed, which may decrease the effective ligand concentration as time.

We have previously demonstrated the formation of step-growth gels using a visible light source and with a single initiator component eosin-Y.^{35,36} We found that eosin-Y deprotonates thiols to generate thiyl radicals, which propagate through cyclic olefin moieties on four-arm PEG-norbornene and cause rapid gel cross-linking (gel point ~20 s). We have also shown that eosin-Y and multifunctional thiols could be used to initiate mixed-mode step-and-chain-growth gelation using multiarm vinyl-based PEG macromers, including PEG-tetra-acrylate (PEG4A) and PEG-tetra-acrylamide (PEG4AA).³⁷ This mixed-mode gelation was further accelerated by adding a small amount of co-monomer NVP (0.1% or 9.4 mM). The use of PEG4A as the macromer resulted in hydrogels that could be degraded hydrolytically while PEG4AA cross-linked hydrogels remained hydrolytically stable for several weeks *in vitro*. The degradation of PEG4A hydrogels followed pseudo-first order hydrolysis kinetics and the degradation rate could be readily tuned by adjusting the concentration of co-monomer NVP. Because this gelation scheme does not use TEA, it is highly cyto-compatible for *in situ* encapsulation, *in vitro* culture, and osteogenic differentiation of human mesenchymal stem cells (hMSCs).³⁷

In this contribution, we aimed at expanding the applicability of this visible light initiated mixed-mode step-and-chain growth gelation scheme by using inexpensive and widely available linear macromer PEGDA. We examined the effects of various parameters on the gelation of visible light cured PEGDA-based thiol-acrylate hydrogels. We further evaluated the impact of pendant peptide functionality (e.g., acrylated or cysteine-bearing peptide) on peptide immobilization efficiency, as well as its influence on gel cross-linking. We also studied the influence of gel formulations on hydrolytic degradation and found a high correlation between thiol-content and gel degradation rate. Finally, we demonstrated high cyto-compatibility of this new class of hydrogels via *in situ* encapsulation and *in vitro* culture of hepatocellular carcinoma cells (Huh7) in three-dimensions.

MATERIALS AND METHODS

Materials

Eosin-Y disodium salt was purchased from MP Biomedical. Triethanolamine (TEA) and N-vinylpyrrolidone (NVP) were obtained from Alfa Aesar and Acros Organics, respectively. Dithiothreitol (DTT) was purchased from Thermo Fisher. PEGs (2, 3.4, and 10 kDa) were obtained from Sigma-Aldrich. Fmoc-amino acids and peptide synthesis reagents were purchased from Chempep or Anaspec. HPLC grade acetonitrile and water were acquired from Thermo Fisher and VWR international, respectively. DMEM and DPBS were purchased from Thermo Fisher. All reagents for cell culture and live/dead staining were obtained from Life Technologies. AlamarBlue cell viability/metabolic indicator was procured from AbD Serotec. QuantiChrom™ urea assay kit was purchased from BioAssay Systems. All other chemicals were acquired from Sigma-Aldrich unless otherwise noted.

Synthesis of PEG-diacrylate (PEGDA)

PEG-diacrylate (PEGDA) was synthesized according to an established protocol.¹⁰ Briefly, PEG-hydroxyl (PEG-OH) was dried azeotropically in anhydrous toluene under nitrogen. After cooling the PEG/toluene solution to room temperature, triethylamine (8 eq.) was added slowly with stirring. Acryloyl chloride (8 eq. of OH group on PEG) dissolved in excess amount of anhydrous toluene was added drop-wise to PEG/toluene solution through an addition funnel. The reaction was stirred overnight at room temperature in the dark and under nitrogen atmosphere. Next, the solution was filtered through neutral aluminum oxide (to remove triethylamine salt) into a flask containing sodium carbonate. The heterogeneous solution was stirred for 2 hr, followed by filtration through a thin layer of Hyflo. The volume of the clear PEGDA solution was reduced by rotovap and precipitated in cold ether. All PEGDA macromers were characterized by ¹H NMR (AVANCE Bruker 500) and the degree of functionalization was at least 95%.

Peptide synthesis and purification

All peptides were built on Fmoc-Rink amide-MBHA resin using standard solid phase peptide synthesis in a microwave peptide synthesizer (CEM Discover). Two sequences were first prepared: CRGDS and RGDS. Following the removal of N-terminal Fmoc group, CRGDS was acetylated by treating the resin-bound peptide with acetic anhydride for 30 min while RGDS was acrylated by coupling the resin-bound peptide with acrylic acid following standard HBTU/HOBt chemistry. The modified peptides (Ac-CRGDS and Acryl-RGDS) were cleaved from the resin in a microwave peptide synthesizer using a cleavage cocktail containing 95% trifluoroacetic acid, 2.5% triisopropylsilane, 2.5% water, and 5 wt % phenol. Cleaved peptides were precipitated and wash three times in cold ether. Preparative reverse phase HPLC (RP-HPLC) (PerkinElmer Flaxer) was used to purify the peptides to at least 90% pure.

Hydrogel fabrication

Mixed-mode step-chain growth PEGDA hydrogels were formed by visible light mediated thiol-acrylate photopolymer-

ization. Prepolymer solutions were prepared by mixing the required components in pH 7.4 PBS: (1) macromer PEGDA, (2) photosensitizer eosin-Y, (3) bifunctional co-initiator DTT, (4) co-monomer NVP, and (5) pendant peptide at desired final concentrations (i.e., 1 mM). Note that all concentrations indicated were final concentrations in the prepolymer solutions. The prepolymer solution was injected between two glass slides separating by two 1 mm Teflon spacers and exposed under halogen cold light (400–700 nm, AmScope, Inc.) for 5 min at 70 k Lux. In some controlled experiments, TEA was used as a co-initiator to yield purely chain-growth nondegradable PEGDA hydrogels.

Rheometry

In situ gelation and real time photo-rheometry were conducted in Bohlin CVO digital rheometer to determine gel points, which were the times at which storage moduli (G') surpassed loss moduli (G''). Briefly, prepolymer solution was placed in a light cure cell and was irradiated through a quartz plate through a flexible light guide. Time-sweep rheometry was operated at 10% strain, 1 Hz frequency, 0.1N normal force, and 90 μ m gap size. Visible light was turned on 15 s after starting the time-sweep measurement. Hydrogel shear moduli were also measured to reveal gel stiffness and hydrolytic degradation as a function of time. Before the measurements, hydrogel discs (8 mm in diameter) were punched out from the gel slabs and incubated in pH 7.4 PBS at 37°C. At predetermined time intervals, the storage (G') and loss (G'') moduli of the hydrogel discs were characterized by oscillatory rheometry operating in strain-sweep (0.1–5%) mode. Gel moduli were measured using a parallel plate geometry (8 mm) with a gap size of 800 μ m.

Peptide incorporation efficiency

The incorporation efficiency of pendant peptide (Ac-CRGDS or Acryl-RGDS. Underlines indicate cross-linkable moieties) in the hydrogel was characterized by analytical RP-HPLC. In addition to the necessary macromer and initiator components, peptide Ac-CRGDS or Acryl-RGDS was added in the prepolymer solution at 1 mM. Peptide-immobilized hydrogels (25 μ L each gel) were prepared via the same visible light exposure as described above. The use of Ac-CRGDS or Acryl-RGDS led to a mixed-mode step-chain growth or a purely chain growth polymerization mechanism, respectively. After gelation, samples were incubated in 200 μ L ddH₂O in microtubes kept at 37°C on an orbital shaker for 1 to 4 days. The solutions were then removed from microtubes and subjected to analytical RP-HPLC to determine the concentration of the released peptide. A series of peptide solutions with known concentrations were analyzed to generate standard curves, which were used to determine the concentration of the released peptide. Peptide incorporation efficiency was determined by mass balance calculation.

Cell culture, encapsulation, and assays

A hepatocyte-derived cellular carcinoma cell line Huh7 was used to evaluate the cytocompatibility of PEGDA-DTT hydrogels formed by visible light mediated thiol-acrylate

photopolymerization. Huh7 cells were maintained in high glucose DMEM containing 10% fetal bovine serum (FBS) and 1× Antibiotic-Antimycotics. Culture media were changed every two to three days. Cell encapsulation was achieved by mixing trypsinized single cells in the prepolymer solutions to a final cell density of 1.5×10^6 cells/mL. Twenty microliters of cell-containing prepolymer solution was injected to a 1 mL syringe with open tip, followed by visible light exposure using the same light source and conditions as described in the previous section. Cell-laden hydrogels were cultured in the same culture media as described above. Cell viability and metabolic activity was determined by Live/Dead staining and AlamarBlue reagent assay (10% in culture media). For live/dead staining, cell-laden gels were incubated in buffer containing Calcein AM (0.25 μ L/mL, stained live cells green) and Ethidium homodimer-III (2 μ L/mL, stained dead cells red) for 1 h. Stained cell-laden gels were rinsed with DPBS briefly before imaging using a confocal microscope (Olympus Fluoview, FV1000). At least three sets of images per gel sample were taken (100 μ m thick, 10 μ m per slice). For metabolic activity assay, cell-laden gels were incubated in 10% AlamarBlue solution for 4 hr and the fluorescence generated were analyzed by a microplate reader (excitation: 560 nm and emission: 590 nm). Cell culture media containing urea secreted by the encapsulated cells over a period of 18 hr were collected at day 1, 4, and 7. Urea quantification was conducted using QuantiChrom™ Urea Assay Kit following manufacture's instructions. Fresh cell culture medium was used as blank control.

Statistics

All statistical analyses and curve fittings were conducted using GraphPad Prism 5 software. Gel swelling (with more than three experimental groups), cell metabolic activity, and urea secretion were analyzed by two-way ANOVA followed by Bonferroni's *post hoc* test with control group specified in the respective figure captions. Gel points and swelling ratio with single experimental group were analyzed by one-way ANOVA followed by Turkey *post hoc* test. All experiments were conducted independently for at least three times. Data presented were Mean \pm SD. Single, double, and triple asterisks represent $p < 0.05$, 0.01, and 0.001, respectively. $p < 0.05$ was considered statistically significant.

RESULTS AND DISCUSSION

Effect of eosin-Y on visible light initiated thiol-acrylate gelation

We have previously shown that PEG-based hydrogels can be prepared by visible light initiated photo-crosslinking using photosensitizer eosin-Y, multiarm macromer PEG-tetraacrylate or PEG-tetra-acrylamide, and bi-functional thiol co-initiator/cross-linker (DTT or *bis*-cysteine-bearing peptides).³⁷ The objectives of this study were to: (1) expand the applicability of this visible light mediated gelation by using linear PEGDA as the macromer; (2) understand the effect of various parameters on gelation and degradation of this new class of hydrogels; and (3) evaluate the potential of this gel platform for *in situ* encapsulation, culture, and

differentiation of hepatocytes (Huh7). We hypothesized that gelation will occur with the use of linear macromer PEGDA and bi-functional thiol co-initiator DTT in the presence of visible light exposure and non-cleavage type initiator eosin-Y. As shown in Figure 1(A), under visible light exposure thiol radicals generated by eosin-Y attack vinyl groups on PEGDA to form carbon radicals. These carbon radicals either propagate through other acrylates (i.e., chain-growth homopolymerization) or further abstract hydrogen from other thiols (i.e., step-growth thiol-acrylate reaction). These visible light mediated polymerization steps yielded a mixed-mode step-chain-growth network structure that is similar to the gels fabricated from UV-mediated thiol-vinyl polymerizations.^{17,38–40} Figure 1(B) shows the influence of eosin-Y on the appearance of PEGDA thiol-acrylate hydrogels prepared from 10 wt % PEGDA (3.4 kDa), eosin-Y (0.025, 0.05, or 0.1 mM), 10 mM DTT (i.e., 20 mM SH_{DTT}), and 0.1% NVP (or 9.4 mM). Although the use of 0.1 mM eosin-Y caused the gels to appear slightly in red post-gelation (5 min visible light exposure), the gels became mostly transparent after incubating in PBS overnight. The gels also appeared larger in size after overnight incubation in pH 7.4 PBS. To determine gelation kinetics, we conducted *in situ* photorheometry using the same macromer compositions. We found that gel points decreased from 249 ± 14 s to 156 ± 3 and 125 ± 11 s when eosin-Y concentration was increased from 0.025 mM to 0.05 and 0.1 mM, respectively [Fig. 1(C)]. While further increasing eosin-Y concentration will accelerate gelation kinetics, higher degree of light attenuation will likely occur and affect the gelation efficiency in thicker gel samples.³⁵ These gel points were slower than the visible light initiated thiol-norbornene reaction that we previously reported (5–20 s) and were similar to that in UV-mediated chain-growth polymerization of PEGDA hydrogels.⁴¹ Figure 1(D) shows the results of strain-controlled rheometry experiments. The storage moduli (G') of these hydrogels were at least one order of magnitude higher than the respective loss moduli (G''), indicating the formation of elastic gels with tunable stiffness ($G' \sim 0.4$, 1.4, and 1.8 kPa for gels formed with 0.025, 0.05, and 0.1 mM, respectively). The improvement in gel crosslinking at higher eosin-Y concentrations could also be observed in hydrogel swelling. Figure 1(E) shows that the equilibrium mass swelling ratios (Q_m) of PEGDA-DTT hydrogels decreased as increasing eosin-Y concentration in the prepolymer solution.

The mechanism of this visible light initiated thiol-acrylate gelation is different from purely chain-growth acrylate homopolymerization or purely step-growth thiol-norbornene reaction. In our current system, gelation was initiated by thiol radicals generated by proton extraction (by photo-excited eosin-Y) and the presence of thiol functionality permits chain-transfer events, which decrease the molecular weights of polyacrylate kinetic chains. In the purely radical mediated step-growth thiol-norbornene gelation system, the cross-linking was not inhibited by oxygen and therefore reached gel points faster than the current system. This gelation is similar to the UV-initiated gelation methods developed by Salinas and Bowman.^{17,38–40,42} The

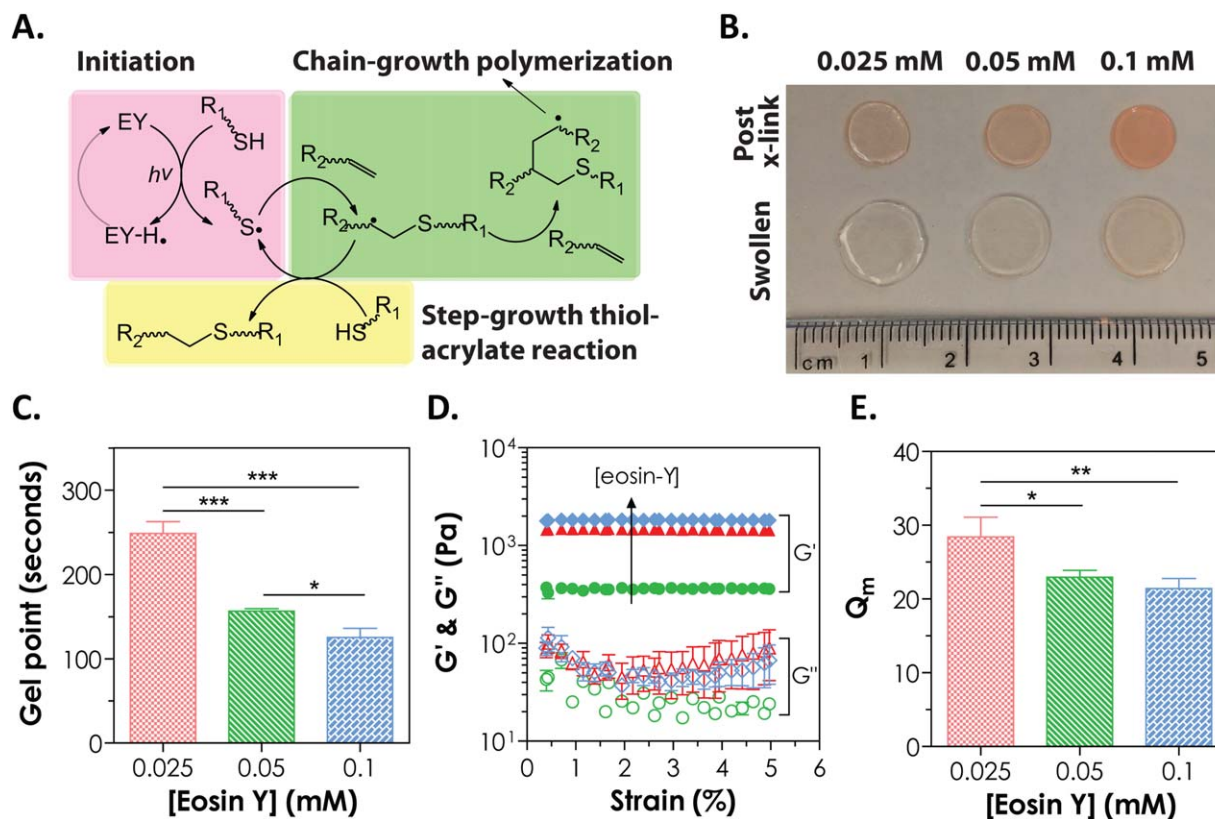


FIGURE 1. A: Mechanism of visible light initiated mixed-mode step-chain-growth thiol-acrylate photopolymerization. B–E: Physical properties of visible light cured PEGDA thiol-acrylate hydrogels formed with 0.025, 0.05, or 0.1 mM of eosin-Y. (B) Photographs; (C) Gel points; (D) Elastic (G') and viscous (G'') modulus, and (E) Equilibrium mass swelling ratio (Q_m). All properties were measured at day 1 postgelation. All gels were prepared from 10 wt % PEGDA (3.4 kDa) with 10 mM DTT (or 20 mM [SH]_{DTT}) and 0.1% NVP, and with 5 min visible light exposure ($N=3$, mean \pm SD, * $p < 0.05$, ** $p < 0.01$, *** $p < 0.001$). [Color figure can be viewed in the online issue, which is available at wileyonlinelibrary.com.]

major difference between the gelation mechanism proposed here and the previous thiol-acrylate gelation systems is that a more cytocompatible visible light source and a noncleavage type initiator were used. Furthermore, because of the use of eosin-Y and visible light, thiyl radicals provided by the bifunctional thiols (e.g., DTT) were the only radical source capable of initiating gelation. In prior systems where a cleavage type initiator (e.g., I-2959) was used, gelation might also be initiated via homopolymerization of acrylates. When comparing our system with the conventional visible light initiated gelation where triethanolamine (TEA) was used as a co-initiator, our system uses bifunctional thiols that not only serve as a more cytocompatible co-initiator but also render the resulting gels degradable due to the formation of hydrolytically labile thiol-ether-ester bonds (see sections below).

Effect of PEGDA molecular weight and thiol-content on stiffness of thiol-acrylate hydrogel

We also evaluated the effect of PEGDA molecular weight and bifunctional thiol (i.e., [SH]_{DTT}) content on the shear moduli of these visible light cured thiol-acrylate hydrogels in their equilibrium swelling state (at day 1 postgelation). PEGDA with molecular weights of 2, 3.4, or 10 kDa and concentrations of 10 or 15 wt % were used. We found that

there was a parabolic relationship between the biofunctional thiol concentration in the prepolymer solution and the shear moduli of the resulting hydrogels for all PEGDA molecular weights used (Fig. 2). Furthermore, the bifunctional thiol concentration required to reach maximum gel modulus shifted to a higher value as the molecular weight of PEGDA decreases. For example, when 10 kDa PEGDA at 10 wt % was used, the concentration of bifunctional thiol needed to reach highest gel modulus was 5 mM (corresponding to 2.5 mM DTT). When 3.4 or 2 kDa PEGDA macromers were used (also at 10 wt % but with higher molar concentrations, Table I), the concentrations of bi-functional thiols required for reaching highest gel stiffness increased to 20 or 60 mM (10 or 30 mM DTT), respectively. Increasing PEGDA concentration from 10 wt % [Fig. 2(A)] to 15 wt % [Fig. 2(B)] increased not only overall gel stiffness (from ~ 0.6 kPa, 4.6 kPa, or 5.8 kPa to ~ 1.4 kPa, 11.2 kPa, or 11.7 kPa for 10, 3.4, or 2 kDa PEGDA, respectively), but also the range of bifunctional thiol concentrations necessary for obtaining highly cross-linked hydrogels.

In conventional visible light mediated PEGDA gelation, amine-based co-initiator (e.g., TEA) serves only as a co-initiator. In the thiol-acrylate gelation scheme reported here, however, thiol has multiple roles. It is not only a co-initiator that provides thiyl radicals to initiate gelation, but also a

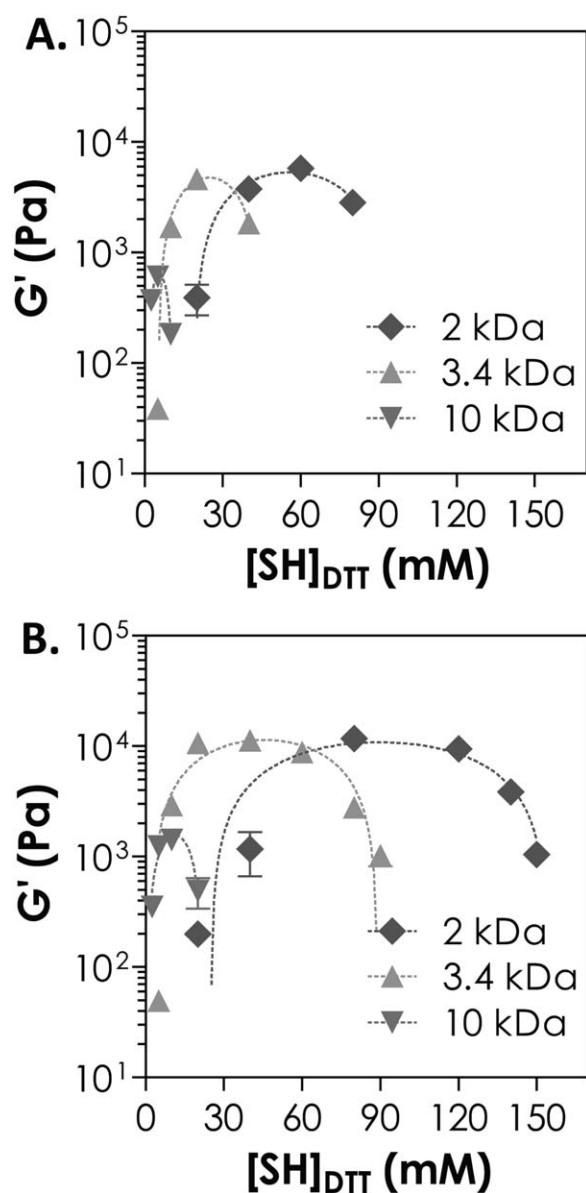


FIGURE 2. Effect of PEGDA molecular weight and bi-functional thiol content on equilibrium shear moduli measured at day 1 postgelation. PEGDA macromers were used at: (A) 10 wt % and (B) 15 wt %. All hydrogels were formed with 0.1 m eosin-Y and 0.1% NVP and with 5 min of visible light exposure. Nonlinear curve fitting was conducted using parabolic relationships as a function of bifunctional thiol content. [Color figure can be viewed in the online issue, which is available at wileyonlinelibrary.com.]

linker and a chain-transfer agent that impact the degree of gel cross-linking. For PEGDA macromer with a particular molecular weight, there is a minimal thiol content or thiol-to-acrylate ratio needed to initiate thiol-acrylate gelation (Table I). Depending on PEGDA molecular weight and weight content, the minimal thiol-to-acrylate ratio needed for initiating thiol-acrylate gelation was between 0.06 and 0.2. Initial increases of thiol content in the prepolymer solution increased gel shear modulus, which was a result of increased thiol radical concentration that accelerated gelation kinetics. However, further increasing thiol-content

resulted in reduction in gel stiffness. Increasing concentration of the bi-functional thiol increased chain-transfer events, which decreased the degree of homopolymerization and the number of high molecular weight polyacrylate chains.⁴² In this scenario, more acrylates participated in the step-growth thiol-acrylate reaction rather than chain-growth polymerization. Since both PEGDA and DTT are linear macromers, theoretically a thiol-to-acrylate ratio of one would result in the formation of linear polymers rather than a cross-linked network. In some examples, however, gelation still occurred at a unity thiol-to-acrylate ratio. This was due to the use of 0.1% NVP (9.4 mM) that decreased overall thiol/vinyl ratio (Table I). It is worth noting that the use of a bi-functional thiol molecule (e.g., DTT) is essential because we have shown that mono-thiol (i.e., cysteine) could not initiate gelation within a short period of time.³⁷

Effect of pendant peptide functionality on peptide immobilization efficiency and gel stiffness

Covalent immobilization of bioactive motifs in a hydrogel network has become a routine and necessary task when designing hydrogels for cell studies. High peptide immobilization efficiency is critical, especially for *in situ* cell encapsulation, because soluble peptides compete with the immobilized ones for cell surface receptors and reduce the efficacy of immobilized peptides. Another criterion pertaining to the incorporation of pendant peptide is that it should not affect gelation efficiency. We evaluated the influence of pendant peptide incorporation on the properties of visible light cured PEGDA thiol-acrylate hydrogels at various bifunctional thiol contents (Fig. 3). Gels were either prepared without pendant peptide (blank) or with 1 mM of acetylated-CRGDS (Ac-CRGDS) or acrylated-RGDS (Acryl-RGDS). For all conditions tested, gel fraction increased as increasing bifunctional thiol concentration. The incorporation of pendant peptide (either Ac-CRGDS or Acryl-RGDS) had minimal effect on gel fraction only when the concentration of bifunctional thiol was low [10 mM $[SH]_{DTT}$, Fig. 3(A)]. At higher bifunctional thiol contents (i.e., 15, 20, 30 mM $[SH]_{DTT}$), the presence of functionalized pendant peptide showed various degrees of influence on gel fraction. The incorporation of pendant peptides, however, did not affect the overall increasing trend of gel fraction at higher $[SH]_{DTT}$. We also examined pendant peptide immobilization efficiency using analytical RP-HPLC. Peptide-immobilized hydrogels were incubated in distilled water to permit the release of unimmobilized peptide from the gels. As shown in Figure 3(B), the immobilization efficiency of Ac-CRGDS peptide via step-growth thiol-acrylate reaction was consistently high (87–90%) and unaffected by the concentration of bi-functional thiol linker incorporated in the prepolymer solution. The immobilization efficiency of Acryl-RGDS via chain-growth polymerization, however, was much lower (33–67%) and somewhat fluctuated depending on the concentration of bi-functional thiol linker. Increasing gel incubation time for peptide leaching from 1 to 4 days did not significantly change the results (data not shown). The low immobilization efficiencies of acrylated peptides in visible light initiated chain-growth polymerized network have been

TABLE I. Formulations of Visible Light Curable PEGDA Hydrogels with DTT as a Bifunctional Co-initiator

PEGDA (wt %)	PEGDA m.w. (Da)	Acrylate (mM)	[SH] _{DTT} (mM) ^a	[SH]/[acrylate]	[SH]/[vinyl] ^b
10	2,000	100	20–80	0.2–0.8	0.183–0.734
	3,350	60	5–40	0.08–0.67	0.072–0.580
	10,000	20	2.5–10	0.13–0.5	0.086–0.345
15	2,000	150	20–150	0.13–1	0.126–0.943
	3,350	90	5–90	0.06–1	0.051–0.909
	10,000	30	2.5–20	0.08–0.67	0.064–0.513

^a[SH]_{DTT} represents thiol concentration, with is twice the concentration of DTT.

^b[Vinyl] = [acrylate] + [NVP]. All gel formulations contain 9.4 mM (0.1 vol %) NVP.

reported in the literature (23–66%).^{12,43} Salinas and Anseth have also reported high peptide immobilization efficiency (85–95%) in UV-based thiol-acrylate polymerization.¹⁷ Our

visible light mediated thiol-acrylate polymerization also yielded high degree of peptide immobilization, likely due to higher reactivity between thiol and acrylate moieties.

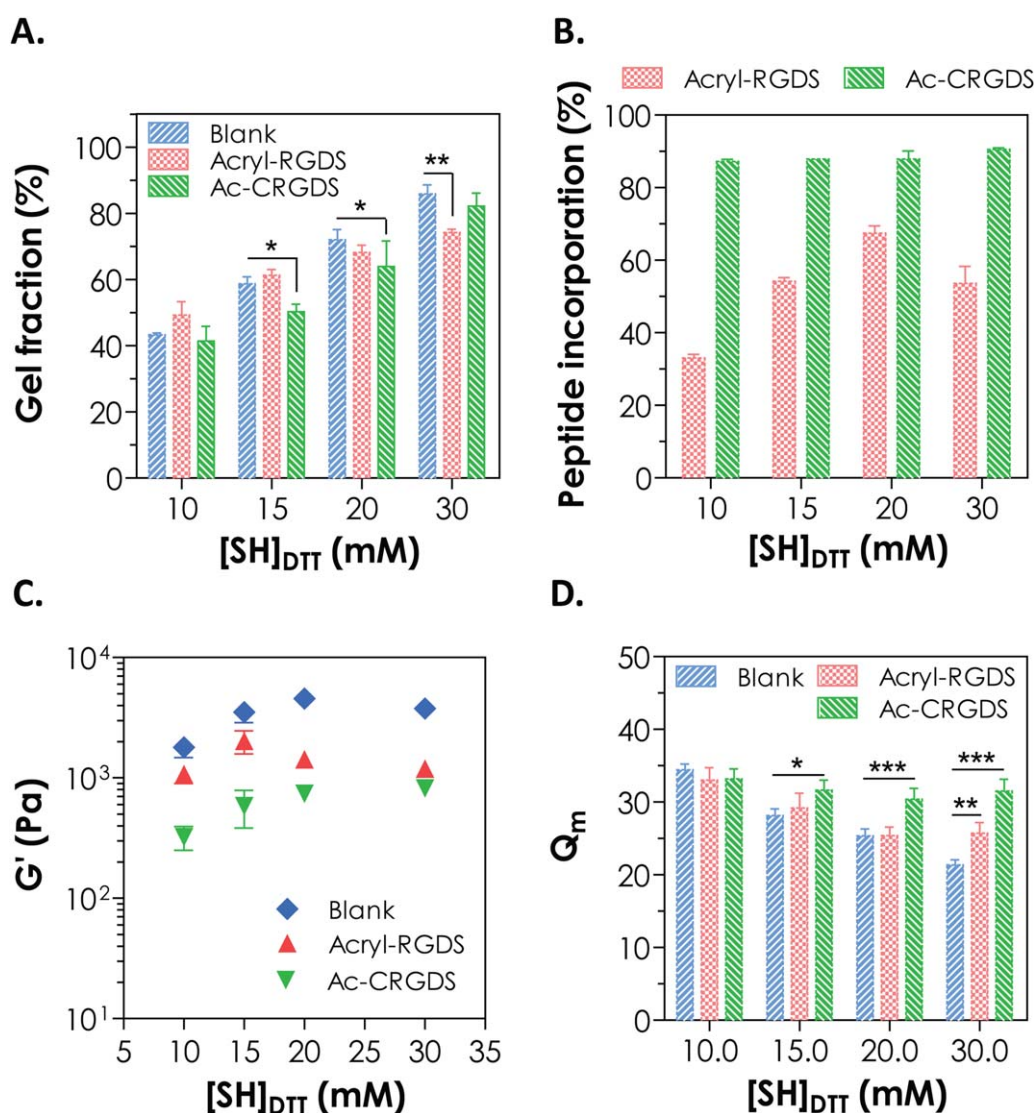


FIGURE 3. Effect of pendant peptide (i.e., Acryl-RGDS or Ac-CRGDS) and bi-functional thiol content on: (A) gel fraction, (B) peptide immobilization efficiency, and (C) equilibrium shear moduli (measured at day 1 postgelation). All gels were prepared by 10 wt % PEGDA_{3.4kDa}, 0.1 mM eosin-Y, 0.1% NVP, and with 5 min visible light exposure. All peptides were incorporated at 1 mM in the prepolymer solutions. Gels containing no pendant peptide (i.e., Blank) were used as control for statistical analysis ($N = 3$, mean \pm SD, * $p < 0.05$, ** $p < 0.01$). [Color figure can be viewed in the online issue, which is available at [wileyonlinelibrary.com](http://www.interscience.wiley.com).]

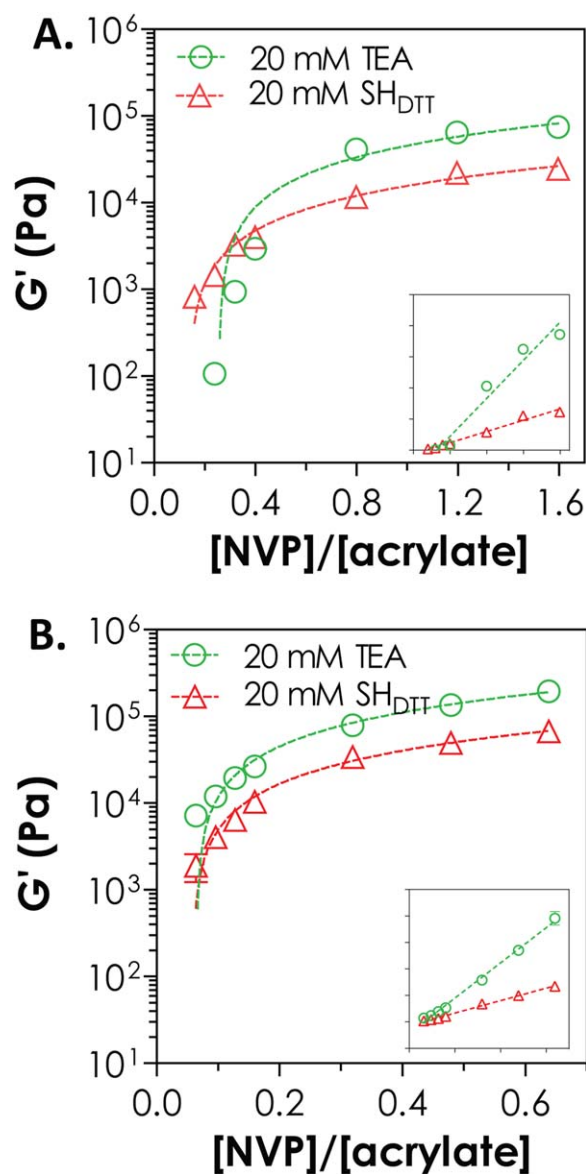


FIGURE 4. Effect of $[NVP]/[acrylate]$ on hydrogel equilibrium shear moduli (measured at day 1 postgelation). Hydrogels were cross-linked by chain-growth photopolymerization (20 mM TEA as co-initiator) or mixed-mode thiol-acrylate photopolymerization (20 mM bifunctional thiol as co-initiator) using (A) 10 wt % and (B) 25 wt % PEGDA_{3.4}kDa. All gels were prepared with 0.1 mM eosin-Y, 1 mM Ac-CRGDS, and with 5 min of visible light exposure. The concentrations of NVP were 0.1, 0.15, 0.2, 0.25, 0.5, 0.75, and 1 vol % ($N=3$, mean \pm SD). [Color figure can be viewed in the online issue, which is available at wileyonlinelibrary.com.]

The immobilization of pendant peptides negatively affected the shear moduli of the hydrogels, especially in the mixed-mode polymerized gels with lower bifunctional thiol contents (e.g., 10–20 mM) [Fig. 3(C)]. Specifically, the addition of Acryl-RGDS caused 20 to 40% reduction of gel stiffness, whereas the incorporation of Ac-CRGDS reduced gel stiffness by 30 to 60%. Turturro et al. has reported similar reduction in gel stiffness when acrylated peptide was co-copolymerized in TEA-mediated chain-growth PEGDA hydrogels.²² Our results show that the incorporation of

pendant cysteine-bearing peptide caused more reduction in gel stiffness. The incorporation of higher thiol-content in this visible light initiated mixed-mode gelation likely caused higher degree of chain transfer [Fig. 1(A)] that reduces the cross-linking density of the hydrogel (Fig. 2).

Effect of NVP on stiffness of thiol-acrylate hydrogel

Since incorporating pendant peptide negatively affected the degree of gel cross-linking in these visible light cured PEGDA hydrogels, we sought methods to improve network cross-linking while still allowing for facile and high efficiency of peptide incorporation. Addition of a small molecular weight monomer NVP has been shown to accelerate the gelation of acrylate-based hydrogels.^{12,43–45} NVP has also been shown to react preferentially with acrylate double bonds and improves acrylate conversion.⁴⁶ The crosslinking of NVP together with PEGDA also yields a co-polymer network that contains additional poly(NVP) kinetic chains, which impact network structure and mechanical properties. Here, we compared the gel moduli in conventional PEGDA/TEA/NVP and the current PEGDA/DTT/NVP gelation systems. Previous study has shown that the molar ratio of NVP to acrylate is a critical parameter affecting final gel stiffness.¹² As shown in Figure 4, increasing $[NVP]/[acrylate]$ ratio indeed caused gels with higher stiffness [PEGDA_{3.4} kDa was fixed at 10 wt % in Fig. 4(A) or 25 wt % in Fig. 4(B)]. We found that there was a linear relationship between the gel shear modulus and $[NVP]/[acrylate]$ ratio for both chain-growth and mixed-mode polymerized hydrogel systems. While Elbert and Hubbell reported this phenomenon for chain-growth networks,¹² we found that the dependency of gel stiffness on $[NVP]/[acrylate]$ ratio was lower in the mixed-mode polymerized gels, as demonstrated by lower slopes in the linear regression analysis (Fig. 4 and Table II). The chain-transfer events occurring in the mixed-mode thiol-acrylate photopolymerization likely reduced the influence of NVP on hydrogel cross-linking density. Nonetheless, increasing NVP concentration from 0.1% to 1.0% increased the shear moduli of 10 wt % PEGDA-DTT hydrogels from 0.8 kPa to 25 kPa, a range suitable for many cell studies.

Effect of macromer formulations on hydrolytic gel degradation

All PEGDA hydrogels prepared in this contribution degraded hydrolytically due to the formation of hydrolytically labile thiol-ether-ester bonds following thiol-acrylate photopolymerization. Figure 5 shows the influence of bi-functional thiol concentration (as indicated by the figure legends) and NVP content [0, 0.1, 1.0% in Fig. 5(A–C), respectively] on

TABLE II. Linear Regression Results of Data Presented in Figure 4

PEGDA (wt %)	Co-Initiator	Slope	R^2
10	20 mM TEA	61,190 \pm 3085	0.96
	20 mM SH _{DTT}	18,090 \pm 672	0.97
25	20 mM TEA	332,300 \pm 7346	0.99
	20 mM SH _{DTT}	117,600 \pm 2548	0.99

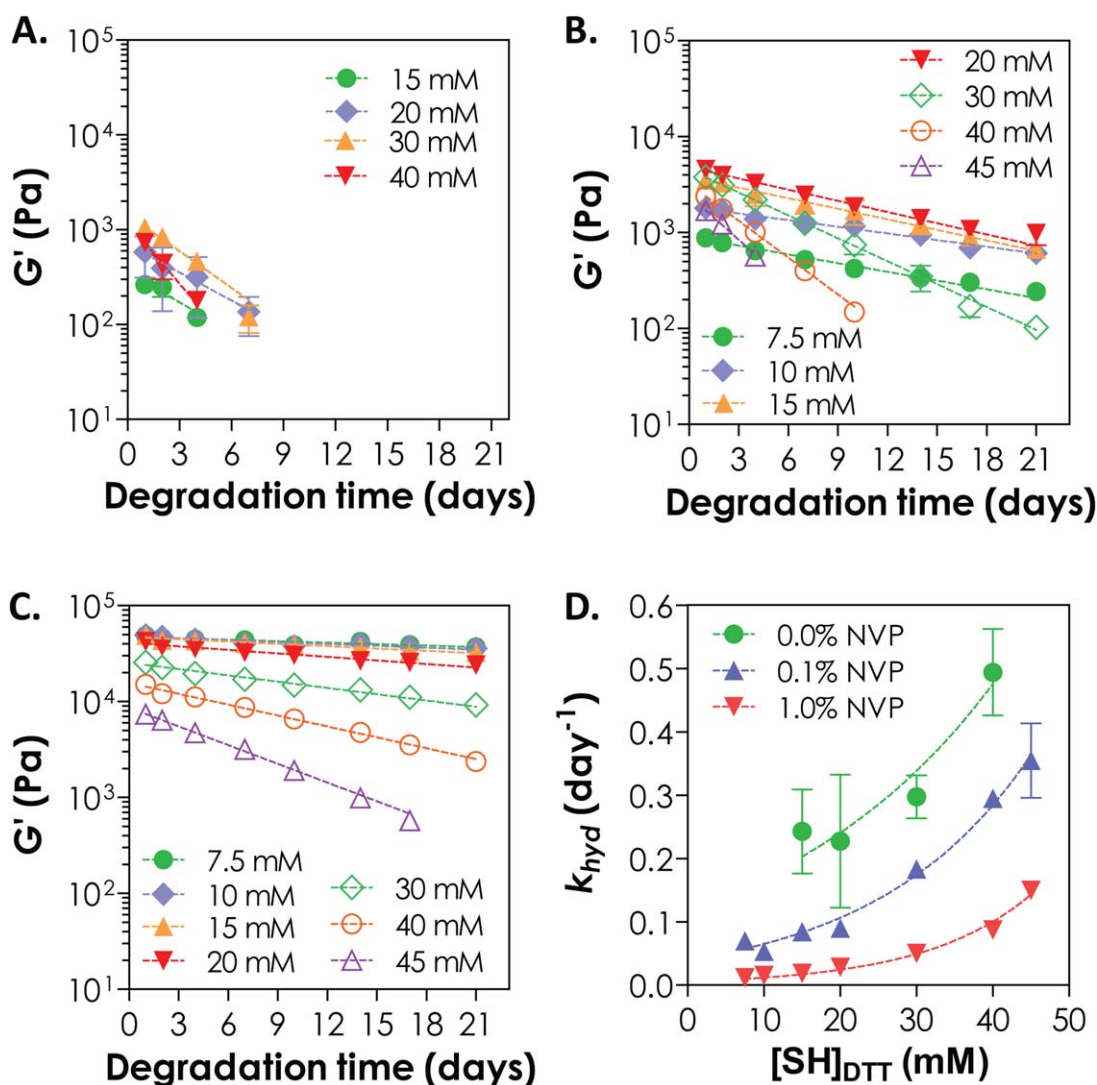


FIGURE 5. Effect of bi-functional thiol concentrations in the prepolymer solution on hydrolytic degradation of mixed-mode PEGDA thiol-acrylate hydrogels. Hydrogel shear moduli were plotted as a function of DTT degradation time. NVP was added at: (A) 0%, (B) 0.1%, and (C) 1.0%. Figure legends indicate total thiol concentrations (i.e., two-fold of DTT concentration). All gels were prepared with 0.1 mM eosin-Y and with 5 min of visible light exposure. All degradation profiles were analyzed using exponential curve fitting (log scale on y-axis). Gel degradation was conducted in pH7.4 PBS at 37°C. (D) Hydrolytic degradation rate constants (k_{hyd}) obtained from (A–C) and plotted as a function of bifunctional thiol concentration. Curves indicate an empirical fitting with an exponential growth relationship ($N = 3$, mean \pm SD). [Color figure can be viewed in the online issue, which is available at wileyonlinelibrary.com.]

shear moduli of PEGDA hydrogels as a function of gel degradation time. Exponential decay curve-fitting results revealed that the degradation of these thiol-acrylate hydrogels followed pseudo-first order hydrolysis kinetics given by:^{31,39,42,47–49}

$$\ln(G'_t) = \ln(G'_0) - k_{hyd} \cdot t \quad (1)$$

Here, G'_0 is the gel modulus before the occurrence of significant degradation and G'_t is the shear modulus at any time during degradation. k_{hyd} is the apparent hydrolytic degradation rate constant (day⁻¹) and t is the degradation time (day). This empirical degradation model has been used to predict the degradation of many hydrogels containing ester or thiol-ether-ester linkages.^{39,42,49} Figure 5 shows

that, at any given NVP and bifunctional thiol concentrations, the degradation rate (k_{hyd}) does not change as a function of time. However, the degradation rate clearly varied depending on the gel formulations. Specifically, all gels containing no NVP degraded rapidly and dissolved completely within one week [Fig. 5(A)]. When NVP was included in the prepolymer solutions at 0.1 vol %, most of the gels remained intact, but weakened as time, for more than 3 weeks, except for gels cross-linked with 40 or 45 mM bifunctional thiol [Fig. 5(B)]. All gels cross-linked with 1 vol % NVP were more stable unless high concentration of bifunctional thiol (e.g., 45 mM) was used [Fig. 5(C)]. To reveal the relationship between k_{hyd} and gel formulations, we plotted the empirically obtained k_{hyd} values against bi-functional thiol concentration for all three NVP concentrations [Fig. 5(D)]. Clearly,

TABLE III. Exponential Fitting of Hydrogel Degradation Rate Constant (k_{hyd}) as a Function of Bifunctional Thiol Concentration at Different NVP Contents

[NVP] (vol %)	Slope	R^2
0	0.034 ± 0.007	0.92
0.1	0.049 ± 0.003	0.99
1.0	0.071 ± 0.006	0.98

k_{hyd} decreases with increasing NVP concentration for all bi-functional thiol concentrations. Since increasing NVP concentration in the prepolymer solution increases poly(NVP) content in the resulting gels, it was possible that these non-degradable and less hydrophilic poly(NVP) chains altered water accessibility to the hydrolytically labile thiol-ether-ester bonds. We further evaluated the dependency of k_{hyd} on bi-functional thiol concentration using non-linear curve fitting and found that the value of k_{hyd} increases exponentially as a function of bi-functional thiol concentration for all three curves. The dependency of k_{hyd} on thiol concentration also has a positive correlation with NVP concentration (Table III). The variation of k_{hyd} in gels with different formations is an interestingly but not completely understood phenomenon. Rydholm et al. observed a similar dependency between k_{hyd} and thiol content in degradable mixed-mode thiol-acrylate and thiol-allylether hydrogels cross-linked by UV light irradiation.^{39,42,49} Using UV-based chain-growth PLA-PEG-PLA block co-polymer hydrogels, Shah et al. also reported dependency of hydrolytic degradation rate to the local hydrogel structure and solvent conditions.³⁰ Although the exact mechanism underlying the dependency of k_{hyd} on gel composition was not clear, the existence of an exponential growth relationship between k_{hyd} and bifunctional thiol (i.e., $[\text{SH}]_{\text{DTT}}$) suggests a predictable way of manipulating gel degradation. Most importantly, many of the current thiol-acrylate hydrogels have gel stiffness (0.8–49 kPa) and degradation rate (1 to several weeks) highly relevant to tissue regeneration applications.

The influence of bifunctional thiol and co-monomer NVP concentrations on the hydrolytic degradation of visible light cross-linked PEGDA hydrogels was also evaluated when 1 mM of Ac-CRGDS peptide was included in the prepolymer solutions [Fig. 6(A–D)]. Conventional visible light cured PEGDA hydrogels with TEA as a co-initiator were used as controls [Fig. 6(E,F)]. PEGDA was used at 10 wt % [Fig. 6(A–C,E)] and 25 wt % [Fig. 6(D,F)]. NVP was added at 0.1, 0.15, 0.2, 0.25, 0.5, 0.75, and 1 vol %, while bifunctional thiol was added at 15 mM [Fig. 6(A)], 20 mM [Fig. 6(B,D)], and 30 mM [Fig. 6(C)]. In controlled experiments, TEA was added at 20 mM for both PEGDA concentrations [Fig. 6(E,F)]. All PEGDA hydrogels cross-linked with bi-functional thiol degraded following the pseudo-first order degradation kinetics as described in Eq. (1). PEGDA thiol-acrylate hydrogels degraded more slowly at higher NVP concentration (>0.5%) or when the gels were cross-linked from 25 wt % PEGDA solution [Fig. 6(D)]. On the contrarily, PEGDA hydrogels cross-linked with TEA as the co-initiator remain hydrolytically stable for all conditions studied [Fig. 6(E,F)].

Exponential curve fitting [Fig. 7(A) and Table IV] revealed good correlations between hydrogel degradation rate constant (k_{hyd}) and NVP concentration ($R^2 = 0.95\text{--}0.97$) for 10 wt % thiol-acrylate PEGDA hydrogels. When the gels were less hydrolytically degradable (i.e., 25 wt % PEGDA), the exponential fitting of k_{hyd} as a function of NVP concentration was less perfect ($R^2 \sim 0.92$). As expected, chain-growth PEGDA hydrogels did not degrade hydrolytically for the duration of the study [Fig. 7(B)]. Another worth-noting difference between thiol-acrylate PEGDA hydrogels and chain-growth PEGDA hydrogels was the influence of co-monomer NVP on gel stiffness (or cross-linking density). In thiol-acrylate PEGDA hydrogels, addition of NVP from 0.1 to 1 vol % caused approximately two orders of magnitude increase in initial gel cross-linking for all formulations tested, regardless of PEGDA concentration. The influence of NVP on chain-growth PEGDA hydrogels, however, depends largely on the concentration of PEGDA in the prepolymer solution. For example, increasing NVP concentration from 0.1 to 1 vol % led to three orders of magnitude increase in gel moduli for 10 wt % PEGDA gels [Fig. 6(E)] but the influence of NVP was less pronounced (increased \sim one order of magnitude) when 25 wt % PEGDA was used [Fig. 6(F)].

PEG hydrogels with tunable degradability are increasingly been developed for tissue engineering applications. However, conventional UV-based or visible light-mediated chain-growth photopolymerization of PEGDA yields hydrogels that are nonhydrolytically degradable in a physiologically relevant time scale. To prepare degradable hydrogels, most approaches available to date rely on the synthesis of degradable macromers having hydrolytically labile segments. Following the synthesis and purification of these degradable macromers, an additional “end-capping” step (acrylation, methacrylation, etc.) is often necessary for obtaining macromers that are cross-linkable. These multi-step material synthesis processes may be labor intensive and time consuming. Further, these custom-designed and synthesized macromers may not be readily available for researchers lacking comprehensive chemical synthesis capacity. From Figures 5 to 7, one can see that hydrogels prepared from PEGDA could be rendered hydrolytically degradable using a single step visible light mediated thiol-acrylate photopolymerization. All components used in this gelation scheme are commercially available yet one can easily tailor the degradation rate of the thiol-acrylate PEGDA hydrogels even without the use of any readily degradable macromer. In our earlier publication, we have also shown that bis-cysteine containing protease-sensitive peptide can be used to render the gels enzymatically degradable.³⁷ This allows one to use simple macromer components to design dynamic multimode degradable hydrogels for *in vitro* 3D cell studies and for *in vivo* tissue regeneration applications.

Three-dimensional culture of hepatocellular carcinoma cells (Huh7) in visible light cured thiol-acrylate hydrogels

Using multiarm PEG-based macromers (PEG-tetra-acrylate and PEG-tetra-acrylamide), we have recently reported the

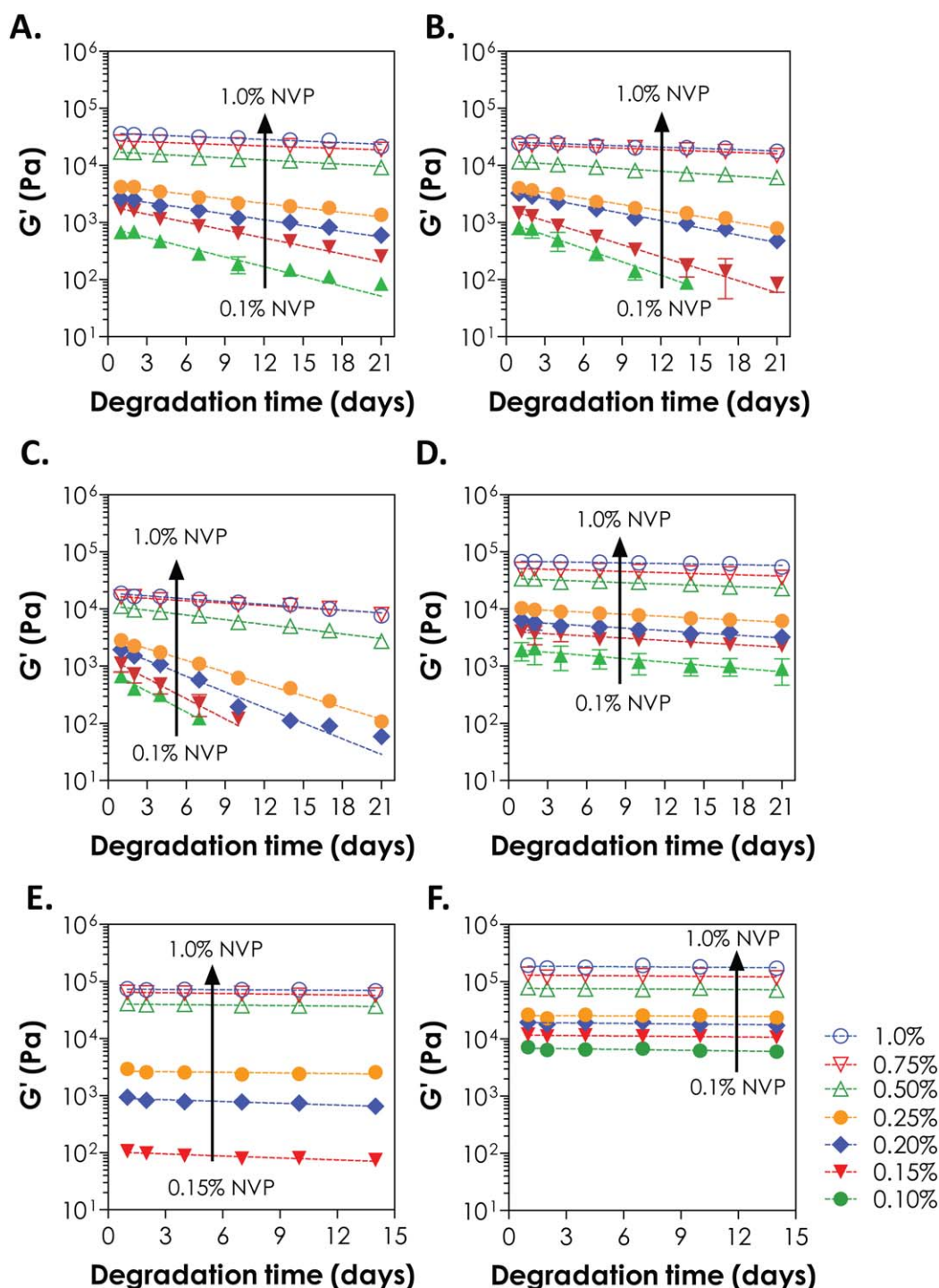


FIGURE 6. Effect of NVP contents on hydrolytic degradation of mixed-mode PEGDA thiol-acrylate hydrogels immobilized with 1 mM Ac-CRGS pendant peptide. Hydrogel shear moduli were plotted as a function of degradation time. Gel formulations are: (A) 10 wt % PEGDA, 15 mM SH_{DTT}; (B) 10 wt % PEGDA, 20 mM SH_{DTT}; (C) 10 wt % PEGDA, 30 mM SH_{DTT}; (D) 25 wt % PEGDA, 20 mM SH_{DTT}; (E) 10 wt % PEGDA, 20 mM TEA; and (F) 25 wt % PEGDA, 20 mM TEA. All gels were prepared with 0.1 mM eosin-Y and with 5 min of visible light exposure. All degradation profiles were analyzed using exponential curve fitting (log scale on y-axis). Gel degradation was conducted in pH 7.4 PBS at 37°C ($n=3$, mean \pm SD). [Color figure can be viewed in the online issue, which is available at wileyonlinelibrary.com.]

cytocompatibility of thiol-vinyl gelation system on the viability and osteogenic differentiation of *in situ* encapsulated human mesenchymal stem cells (hMSCs).³⁷ Here, we encapsulated hepatocellular carcinoma cells Huh7 to evaluate the

potential of this thiol-based visible light initiated PEGDA hydrogels for liver tissue engineering applications. Huh7 cells are immortalized hepatocellular carcinoma cells that, when grown on tissue culture plastics, exhibit flat

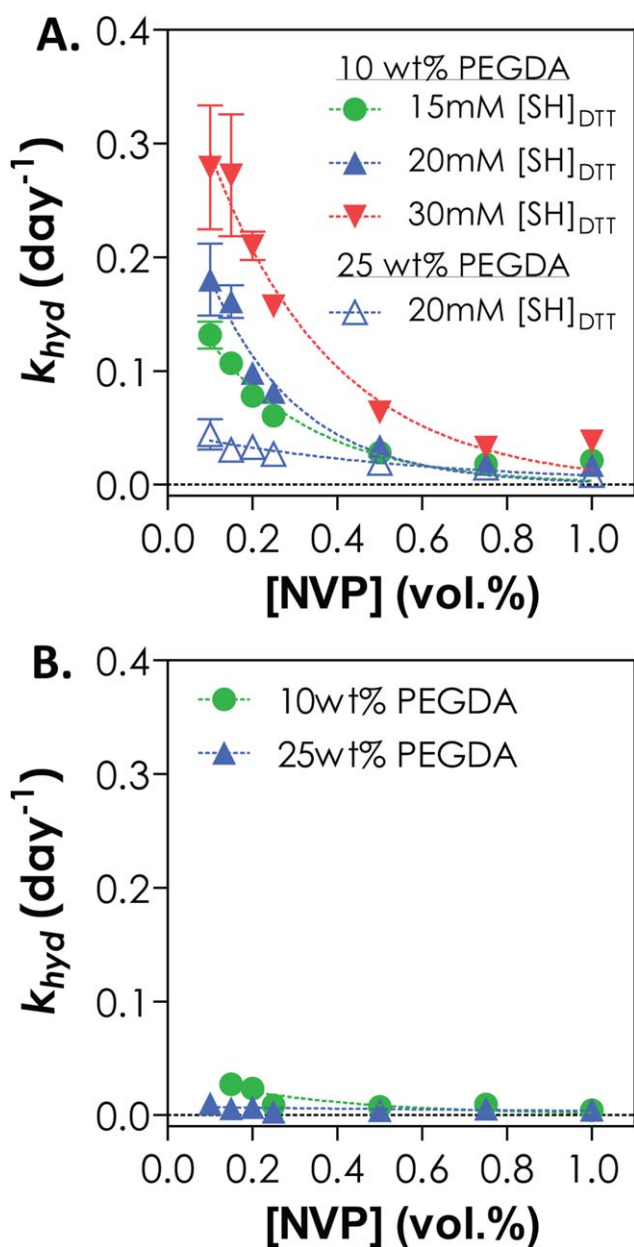


FIGURE 7. Hydrolytic degradation rate constants (k_{hyd}) obtained from Figure 6 and plotted as a function of NVP concentration: (A) mixed-mode PEGDA thiol-acrylate hydrogels, and (B) chain-growth PEGDA hydrogels. Curves indicate an empirical fitting with an exponential decay relationship. [Color figure can be viewed in the online issue, which is available at wileyonlinelibrary.com.]

morphology and proliferate rapidly to form a monolayer.⁵⁰ These cells are commercially available, inexpensive to culture, and are widely used for studying drug toxicity, hepatic gene regulation, and pathogenesis of hepatitis and viral infection. Although these cells are capable of secreting plasma proteins (e.g., albumin), their ability to express functional drug-metabolizing enzymes is not fully characterized.⁵⁰ When cultured on a two-dimensional surface, these cells lose their normal polarity and liver-specific functions. Although a few studies have utilized gel matrices for three-

dimensional culture of Huh7 cells,^{51,52} it remains a challenging task to “differentiate” these cells into functional liver cells that express liver-specific genes including albumin, HNF4 α , α 1-antitrypsin, and CYP450. We hypothesized that our thiol-acrylate hydrogel system can serve as an appropriate gel platform for three-dimensional culture of Huh7 cells (or other hepatocytes). To this end, we encapsulated Huh7 cells (1.5×10^6 cells/mL) in PEGDA hydrogels cross-linked by 30 mM of bifunctional thiol (i.e., 15 mM DTT) and in the presence of different NVP contents (0.1, 0.2, and 0.3 vol %). Figure 8(A) shows the viability (live/dead staining) of Huh7 cells in hydrogels 2-hr (top panel) and 7-day (bottom panel) post-encapsulation. In all gel formulations, vast majority of encapsulated Huh7 cells remained alive for the duration of the study and almost no dead cells were found. Live/Dead staining also revealed that cells proliferated to form small clusters after 7 days of *in vitro* three-dimensional culture. Prior studies have shown that Huh7 cells form clusters naturally when cultured in three-dimensional matrices.^{51,52} As time, these cell clusters would become bigger and our results were similar to these reports [Fig. 8(A)]. We also measured Huh7 cell metabolic activity with Alamarblue reagent and found no difference 1-day postencapsulation for all three cross-linking densities studied [Fig. 8(B)]. Although cell metabolic activity increased over time in all three formulations, Huh7 cells encapsulated in stiffer gels (i.e., 0.2 or 0.3% NVP) exhibited significantly lower metabolic activity [Fig. 8(B)] compared with using gels with lower cross-linking density (i.e., 0.1% NVP). Since cells appeared to remain alive in all gels [Fig. 8(A)] but showed difference in metabolic activity [Fig. 8(B)], we further examined a hepatocellular function—urea secretion—from Huh7 cells encapsulated in gels with different NVP contents [Fig. 8(C)]. As expected, urea secretion from the encapsulated Huh7 cells increased as culture time since cells appeared to form larger clusters after 7 days of *in vitro* culture [Fig. 8(A)]. Interestingly, Huh7 cells encapsulated in gels with higher cross-linking densities (i.e., 0.2 and 0.3 vol % NVP) secreted more urea compared with cells encapsulated in gels with lower cross-linking density (i.e., 0.1% NVP), suggesting improved hepatocellular function in gels with higher cross-linking densities.

The most important criterion of any photoencapsulation system is that cells should retain their viability following the encapsulation process. In this study, we utilized visible light mediated thiol-acrylate photopolymerization to prepare hydrogels with tunable stiffness and degradability for *in situ* encapsulation of Huh7 cells. Following *in situ* photoencapsulation, almost all Huh7 cells remained viable and were able

TABLE IV. Exponential Curve Fitting Results Using Data Presented in Figure 7(A)

[PEGDA] (wt %)	[SH] _{DTT} (mM)	Slope	R ²
10	15	-4.00 ± 0.70	0.95
	20	-4.73 ± 0.78	0.96
	30	-3.47 ± 0.47	0.97
25	20	-1.75 ± 0.32	0.92

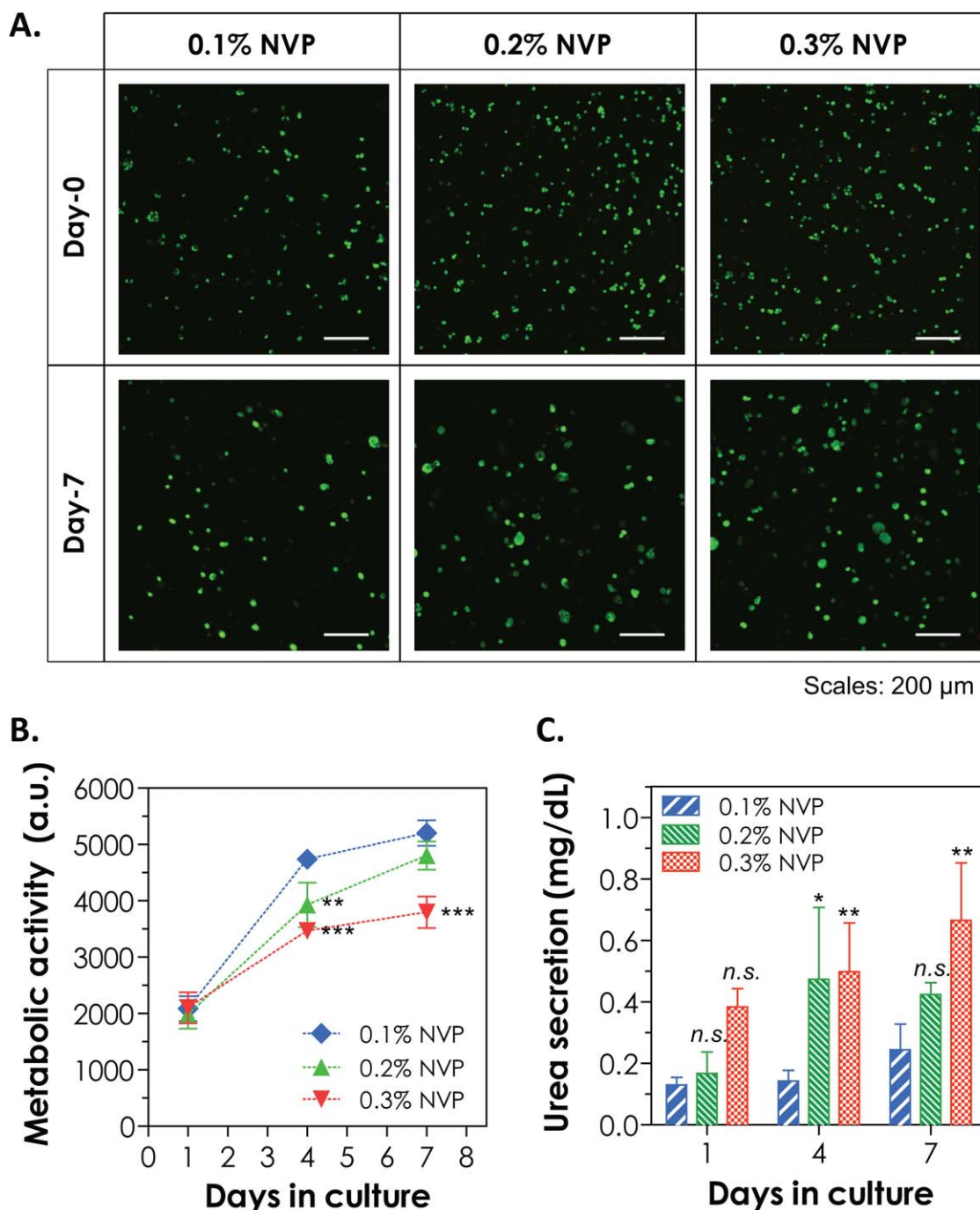


FIGURE 8. Three-dimensional culture of hepatocellular carcinoma cells Huh7 in visible light cured PEGDA thiol-acrylate hydrogels. A: Confocal microscopy images of encapsulated Huh7 cells stained with Live/Dead staining kit (Live cells stained green and dead cells stained red). B: Metabolic activity and (C) urea secretion rate in the encapsulated cells. Cells were encapsulated (1.5×10^6 cells/mL) in 10 wt % PEGDA_{3,4kDa} gels prepared with 0.1 mM eosin-Y, 15 mM DTT, and with 5 min of visible light exposure. All statistical analyses were conducted using 0.1% NVP group (at the same time point) as control ($n = 3$, mean \pm SD, * $p < 0.05$, ** $p < 0.01$, *** $p < 0.001$. n.s.: not significant). [Color figure can be viewed in the online issue, which is available at wileyonlinelibrary.com.]

to proliferate into cell clusters. Gels containing 0.1% NVP had the lowest stiffness and fastest degradation rate. These gels appeared larger than the other two groups (0.2 and 0.3% NVP) due to gel degradation and swelling, which could explain the lower cell counts in the confocal images shown in Figure 8(A). These weakly cross-linked gels (i.e.,

gels with 0.1% NVP) degraded completely within 10 days. Although cells encapsulated in weakly cross-linked gels showed highest metabolic activity and potentially higher degree of proliferation, these hepatocytes showed lower urea secretion as compared with cells encapsulated in stiffer and slow degrading gels [Fig. 8(C)]. Statistical analysis

results show similarity between cell metabolic activity and urea secretion [Fig. 8(B,C)].

One potential explanation accounting for the inverse relationships between urea secretion and cell metabolic activity is that the restricted cell proliferation led to higher degree of differentiation in the encapsulated Huh7 cells. Studies have shown that Huh7 cells cultured in a rotating wall vessel (RWV) bioreactor formed clusters and expressed more hepatocyte-specific transcripts (e.g., HNF4 α , albumin, etc.) than cells cultured in monolayer.⁵³ It is also possible that additional poly(NVP) chains within the hydrogels stimulated the differentiation and urea secretion in the encapsulated Huh7 cells. Polymers containing poly(NVP) have been shown to promote albumin secretion from two-dimensional culture of C3A hepatoblastoma cells.⁵⁴ We are not aware of any three-dimensional study showing the influence of poly(NVP)-containing hydrogels on hepatocyte phenotype and future work will focus on exploring the impact of hydrogel formulations on hepatocyte differentiation for three-dimensional liver regeneration, drug screening, and viral infection.

CONCLUSION

In conclusion, we have shown that multifunctional thiol-based molecules and linear PEGDA macromer can be used to initiate visible light-mediated thiol-acrylate photopolymerization and hydrogel cross-linking. Increasing concentrations of photosensitizer eosin-Y or co-monomer NVP accelerated the thiol-acrylate gelation kinetics. Adjusting bifunctional thiol concentration afforded additional controls in hydrogel cross-linking density. Conditions affecting gelation efficiency also resulted in changes on hydrolytic gel degradation. The hydrolytic degradation of these thiol-acrylate hydrogels followed pseudo-first order degradation kinetics and the degradation rate constants were affected by thiol and NVP contents. Finally, the readily available macromer and initiator components used in this gelation system have high cytocompatibility, as demonstrated by *in situ* Huh7 cell encapsulation. Although almost all cells retained high viability and formed clusters in the thiol-acrylate hydrogels, cell metabolic activity was affected by the concentration of NVP added in the prepolymer solution. The secretion of urea from the encapsulated cells was found to be highly dependent on the gel properties and inversely proportional to cell metabolic activity, suggesting that this system may be useful in promoting higher degree of hepatocellular differentiation.

ACKNOWLEDGMENTS

The authors thank Prof. Guoli Dai (IUPUI Biology Department) for providing Huh7 cells, as well as Drs. Chang Seok Ki, Tsai-Yu Lin, and Ms. Han Shih for their technical assistance.

REFERENCES

1. Lin CC, Anseth KS. PEG hydrogels for the controlled release of biomolecules in regenerative medicine. *Pharm Res* 2009;26:631–643.
2. Lutolf MP, Hubbell JA. Synthetic biomaterials as instructive extracellular microenvironments for morphogenesis in tissue engineering. *Nat Biotechnol* 2005;23:47–55.

3. Slaughter BV, Khurshid SS, Fisher OZ, Khademhosseini A, Peppas NA. Hydrogels in regenerative medicine. *Adv Mater* 2009;21:3307–3329.
4. Tibbitt MW, Anseth KS. Hydrogels as extracellular matrix mimics for 3D cell culture. *Biotechnol Bioeng* 2009;103:655–663.
5. Sawhney AS, Pathak CP, Hubbell JA. Bioerodible hydrogels based on photopolymerized poly(ethylene glycol)-co-poly(alpha-hydroxy acid) diacrylate macromers. *Macromolecules* 1993;26:581–587.
6. Phelps EA, Enemchukwu NO, Fiore VF, Sy JC, Murthy N, Sulchek TA, Barker TH, Garcia AJ. Maleimide cross-linked bioactive PEG hydrogel exhibits improved reaction kinetics and cross-linking for cell encapsulation and *in situ* delivery. *Adv Mater* 2012;24:64–70.
7. DeForest CA, Anseth KS. Cytocompatible click-based hydrogels with dynamically tunable properties through orthogonal photoconjugation and photocleavage reactions. *Nat Chem* 2011;3:925–931.
8. Alge DL, Azagarsamy MA, Donohue DF, Anseth KS. Synthetically tractable click hydrogels for three-dimensional cell culture formed using tetrazine-norbornene chemistry. *Biomacromolecules* 2013;14:949–953.
9. DeForest CA, Polizzotti BD, Anseth KS. Sequential click reactions for synthesizing and patterning three-dimensional cell microenvironments. *Nat Mater* 2009;8:659–664.
10. Hern DL, Hubbell JA. Incorporation of adhesion peptides into nonadhesive hydrogels useful for tissue resurfacing. *J Biomed Mater Res* 1998;39:266–276.
11. Bryant SJ, Nuttelman CR, Anseth KS. Cytocompatibility of UV and visible light photoinitiating systems on cultured NIH/3T3 fibroblasts *in vitro*. *J Biomater Sci Polym Ed* 2000;11:439–457.
12. Elbert DL, Hubbell JA. Conjugate addition reactions combined with free-radical cross-linking for the design of materials for tissue engineering. *Biomacromolecules* 2001;2:430–441.
13. Ward JH, Peppas NA. Preparation of controlled release systems by free-radical UV polymerizations in the presence of a drug. *J Controlled Release* 2001;71:183–192.
14. Lin-Gibson S, Bencherif S, Cooper JA, Wetzel SJ, Antonucci JM, Vogel BM, Horkay F, Washburn NR. Synthesis and characterization of PEG dimethacrylates and their hydrogels. *Biomacromolecules* 2004;5:1280–1287.
15. Lin-Gibson S, Jones RL, Washburn NR, Horkay F. Structure-property relationships of photopolymerizable poly(ethylene glycol) dimethacrylate hydrogels. *Macromolecules* 2005;38:2897–2902.
16. Weber LM, He J, Bradley B, Haskins K, Anseth KS. PEG-based hydrogels as an *in vitro* encapsulation platform for testing controlled beta-cell microenvironments. *Acta Biomater* 2006;2:1–8.
17. Salinas CN, Anseth KS. Mixed mode thiol-acrylate photopolymerizations for the synthesis of PEG-peptide hydrogels. *Macromolecules* 2008;41:6019–6026.
18. Lin CC, Anseth KS. Controlling affinity binding with peptide-functionalized poly(ethylene glycol) hydrogels. *Adv Funct Mater* 2009;19:2325–2331.
19. Bahney CS, Lujan TJ, Hsu CW, Bottlang M, West JL, Johnstone B. Visible light photoinitiation of mesenchymal stem cell-laden bioresponsive hydrogels. *Eu Cells Mater* 2011;22:43–55.
20. Fairbanks BD, Schwartz MP, Bowman CN, Anseth KS. Photoinitiated polymerization of PEG-diacrylate with lithium phenyl-2,4,6-trimethylbenzoylphosphine: Polymerization rate and cytocompatibility. *Biomaterials* 2009;30:6702–6707.
21. Ki CS, Shih H, Lin CC. Facile preparation of photodegradable hydrogels by photopolymerization. *Polymer* 2013;54:2115–2122.
22. Turturro MV, Sobic S, Larson JC, Papavasiliou G. Effective tuning of ligand incorporation and mechanical properties in visible light photopolymerized poly(ethylene glycol) diacrylate hydrogels dictates cell adhesion and proliferation. *Biomed Mater* 2013;8:025001.
23. Sawhney AS, Pathak CP, Hubbell JA. Modification of islet of Langerhans surfaces with immunoprotective poly(ethylene glycol) coatings via interfacial photopolymerization. *Biotechnol Bioeng* 1994;44:383–386.
24. Sawhney AS, Pathak CP, Hubbell JA. Interfacial photopolymerization of poly(ethylene glycol)-based hydrogels upon alginate poly(L-lysine) microcapsules for enhanced biocompatibility. *Biomaterials* 1993;14:1008–1016.

25. Kizilel S, Perez-Luna VH, Teymour F. Photopolymerization of poly(ethylene glycol) diacrylate on eosin-functionalized surfaces. *Langmuir*. 2004;20:8652–8658.
26. Kizilel S, Perez-Luna VH, Teymour F. Mathematical model for surface-initiated photopolymerization of poly(ethylene glycol) diacrylate. *Macromol Theory Simulat* 2006;15:686–700.
27. Kizilel S, Sawardecker E, Teymour F, Perez-Luna VH. Sequential formation of covalently bonded hydrogel multilayers through surface initiated photopolymerization. *Biomaterials* 2006;27:1209–1215.
28. Cruise GM, Hegre OD, Lamberti FV, Hager SR, Hill R, Scharp DS, Hubbell JA. In vitro and in vivo performance of porcine islets encapsulated in interfacially photopolymerized poly(ethylene glycol) diacrylate membranes. *Cell Transplant* 1999;8:293–306.
29. Cruise GM, Hegre OD, Scharp DS, Hubbell JA. A sensitivity study of the key parameters in the interfacial photopolymerization of poly(ethylene glycol) diacrylate upon porcine islets. *Biotechnol Bioeng* 1998;57:655–665.
30. Shah NM, Pool MD, Metters AT. Influence of network structure on the degradation of photo-cross-linked PLA-b-PEG-b-PLA hydrogels. *Biomacromolecules* 2006;7:3171–3177.
31. Metters AT, Bowman CN, Anseth K S. A statistical kinetic model for the bulk degradation of PLA-b-PEG-b-PLA hydrogel networks. *J Phys Chem B* 2000;104:7043–7049.
32. Hudalla GA, Eng TS, Murphy WL. An approach to modulate degradation and mesenchymal stem cell behavior in poly(ethylene glycol) networks. *Biomacromolecules* 2008;9:842–849.
33. Lin CC, Boyer PD, Aimetti AA, Anseth KS. Regulating MCP-1 diffusion in affinity hydrogels for enhancing immuno-isolation. *J Controlled Release* 2010;142:384–391.
34. Lin CC, Anseth KS. Cell-cell communication mimicry with poly(ethylene glycol) hydrogels for enhancing beta-cell function. *Proc Natl Acad Sci USA* 2011;108:6380–6385.
35. Shih H, Fraser AK, Lin CC. Interfacial thiol-ene photoclick reactions for forming multilayer hydrogels. *ACS Appl Mater Interfaces* 2013;5:1673–1680.
36. Shih H, Lin CC. Visible-light-mediated thiol-ene hydrogelation using eosin-Y as the only photoinitiator. *Macromol Rapid Commun* 2013;34:269–273.
37. Hao Y, Shih H, Munoz Z, Kemp A, Lin C. Visible light cured thiol-vinyl hydrogels with tunable degradation for 3D cell culture. *Acta Biomater* 2014;10:104–114.
38. Reddy SK, Okay O, Bowman CN. Network development in mixed step-chain growth thiol-vinyl photopolymerizations. *Macromolecules* 2006;39:8832–8843.
39. Rydholm AE, Bowman CN, Anseth KS. Degradable thiol-acrylate photopolymers: polymerization and degradation behavior of an in situ forming biomaterial. *Biomaterials* 2005;26:4495–4506.
40. Rydholm AE, Reddy SK, Anseth KS, Bowman CN. Controlling network structure in degradable thiol-acrylate biomaterials to tune mass loss behavior. *Biomacromolecules* 2006;7:2827–2836.
41. Lin CC, Raza A, Shih H. PEG hydrogels formed by thiol-ene photo-click chemistry and their effect on the formation and recovery of insulin-secreting cell spheroids. *Biomaterials* 2011;32:9685–9695.
42. Reddy SK, Anseth KS, Bowman CN. Modeling of network degradation in mixed step-chain growth polymerizations. *Polymer* 2005;46:4212–4222.
43. Turturro MV, Papavasiliou G. Generation of mechanical and bio-functional gradients in PEG diacrylate hydrogels by perfusion-based frontal photopolymerization. *J Biomater Sci Polym Ed* 2012;23:917–939.
44. Kizilel S. Mathematical model for microencapsulation of pancreatic islets within a biofunctional PEG hydrogel. *Macromol Theory Simulat* 2010;19:514–531.
45. Moeinzadeh S, Khorasani SN, Ma JY, He XZ, Jabbari E. Synthesis and gelation characteristics of photo-crosslinkable star poly(ethylene oxide-co-lactide-glycolide acrylate) macromonomers. *Polymer* 2011;52:3887–3896.
46. White TJ, Liechty WB, Natarajan LV, Tondiglia VP, Bunning TJ, Guymon CA. The influence of N-vinyl-2-pyrrolidinone in polymerization of holographic polymer dispersed liquid crystals (HPDLCs). *Polymer* 2006;47:2289–2298.
47. Metters A, Hubbell J. Network formation and degradation behavior of hydrogels formed by Michael-type addition reactions. *Biomacromolecules* 2005;6:290–301.
48. Martens P, Metters AT, Anseth KS, Bowman CN. A generalized bulk-degradation model for hydrogel networks formed from multivinyl cross-linking molecules. *J Phys Chem B* 2001;105:5131–5138.
49. Rydholm AE, Reddy SK, Anseth KS, Bowman CN. Development and characterization of degradable thiol-allyl ether photopolymers. *Polymer* 2007;48:4589–4600.
50. Choi S, Sainz B, Corcoran P, Uprichard S, Jeong H. Characterization of increased drug metabolism activity in dimethyl sulfoxide (DMSO)-treated Huh7 hepatoma cells. *Xenobiotica* 2009;39:205–217.
51. Molina-Jimenez F, Benedicto I, Viet LDT, Gondar V, Lavillette D, Marin JJ, Briz O, Moreno-Otero R, Aldabe R, Baumert TF, Cosset FL, Lopez-Cabrera M, Majano PL. Matrigel-embedded 3D culture of Huh-7 cells as a hepatocyte-like polarized system to study hepatitis C virus cycle. *Virology* 2012;425:31–39.
52. Marfels C, Hoehn M, Wagner E, Gunther M. Characterization of in vivo chemoresistant human hepatocellular carcinoma cells with transendothelial differentiation capacities. *BMC Cancer* 2013;13:176.
53. Sainz B, TenCate V, Uprichard SL. Three-dimensional Huh7 cell culture system for the study of Hepatitis C virus infection. *Virology J* 2009;6:103.
54. Krasteva N, Harms U, Albrecht W, Seifert B, Hopp M, Altankov G, Groth T. Membranes for biohybrid liver support systems—Investigations on hepatocyte attachment, morphology and growth. *Biomaterials* 2002;23:2467–2478.